A Friction damping system

Low order behavior and design

Nielsen, Leif Otto; Mualla, Imad H.

Publication date:
2002

Document Version
Publisher's PDF, also known as Version of record

Leif O. Nielsen
Imad H. Mualla

A Friction Damping System
Low order behavior and design

BYG•DTU

DANMARKS
TEKNISKE
UNIVERSITET

DTU

Rapport
BYG•DTU R-030
2002
ISSN 1601-2917
ISBN 87-7877-090-4

A Friction Damping System
Low order behavior and design

Leif O. Nielsen
Imad H. Mualla

Department of Civil Engineering
DTU-bygning 118
2800 Kgs. Lyngby
http://www.byg.dtu.dk

2002

A FRICTION DAMPING SYSTEM
LOW ORDER BEHAVIOUR AND DESIGN

Leif O. Nielsen and Imad H. Mualla[a]

Department of Civil Engineering,
Technical University of Denmark, 2800 Lyngby, Denmark

[a] DampTech ApS, 2800 Lyngby, Denmark

SUMMARY
A friction damping system for reduction of the response of dynamic loaded structures is studied, the key parameters are identified and the design is discussed.

1. INTRODUCTION
A typical building structure as the n-storey frame on Figure 1 is sensitive to horizontal vibration from wind, earthquakes etc. Damping the horizontal displacement difference between neighbouring floors reduce the horizontal vibrations. A damping system, Mualla [1], with this property is considered in the following and the structural behaviour and design is investigated. The nearly bilinear force-displacement behaviour of some versions of the system is an important property from a practical earthquake design point of view, Skinner et al [2]. An optimum design idea is here related to the resonance case, which is preferred for the more complicated earthquake load case Filiatrault and Cherry [3].

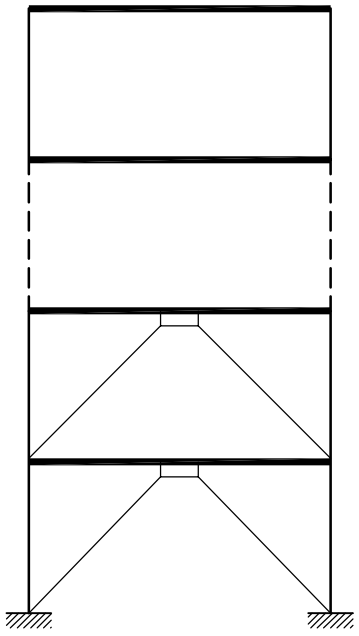

Figure 1. n-storey frame with a damping system in storey 1 and 2.

2. DAMPING SYSTEM
The damping system is investigated in a one-storey frame as shown in Figure 2. This plane frame structure with rigid horizontal beam DAE of length *S* and the bending

flexible vertical columns DF and EG of length H is upgraded with a frictional damping system consisting of a friction damper and a bracing system. The friction damper comprises the rigid beam AC of length h_a and the rigid beam C_1CC_2 of length $2r$ connected by a frictional hinge in C with the frictional moment M_f and an energy dissipation $M_f\,|\dot{\theta}|$, where $\dot{\theta}$ is the time derivative of the angle θ between the rigid beams AC and C_1CC_2. The bracing system comprises the bars FC_1(bar 1) and GC_2(bar 2) of length l pretensioned with the force F_p>0. The friction damper and the bracing system are connected through hinges in the points C_1 and C_2. The damping system is connected to the frame through hinges in point A, F and G. The upgraded frame is symmetric in regard to the vertical line AB. Here is considered that case, where the bar lines go through the hinge A, i.e. the damping system is central, and then

$$\tan v = \frac{h_a}{r} = \frac{H}{S/2} \tag{2.1}$$

where the bar slope angle v is defined on Figure 2.

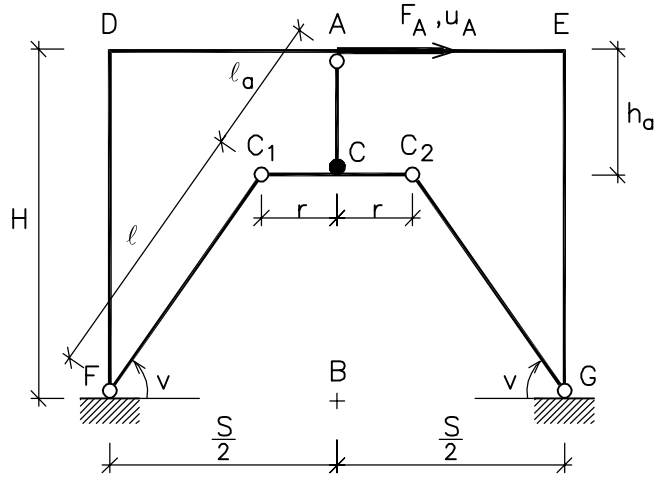

Figure 2. Frame upgraded with friction damping system.

3. ¼ LOAD CYCLE

Important information about the behaviour of the upgraded frame is obtained by loading the frame with a slowly increasing horizontal load F_A in point A. Using a geometric linear structural theory, the antimetrical load F_A gives an antimetrical displacement u_A of point A, i.e. a horizontal displacement.

The section forces in the damping system from the pretension in the bars and from the antimetrical load are shown in Figure 3a respectively 3b using undeformed equilibrium.

.

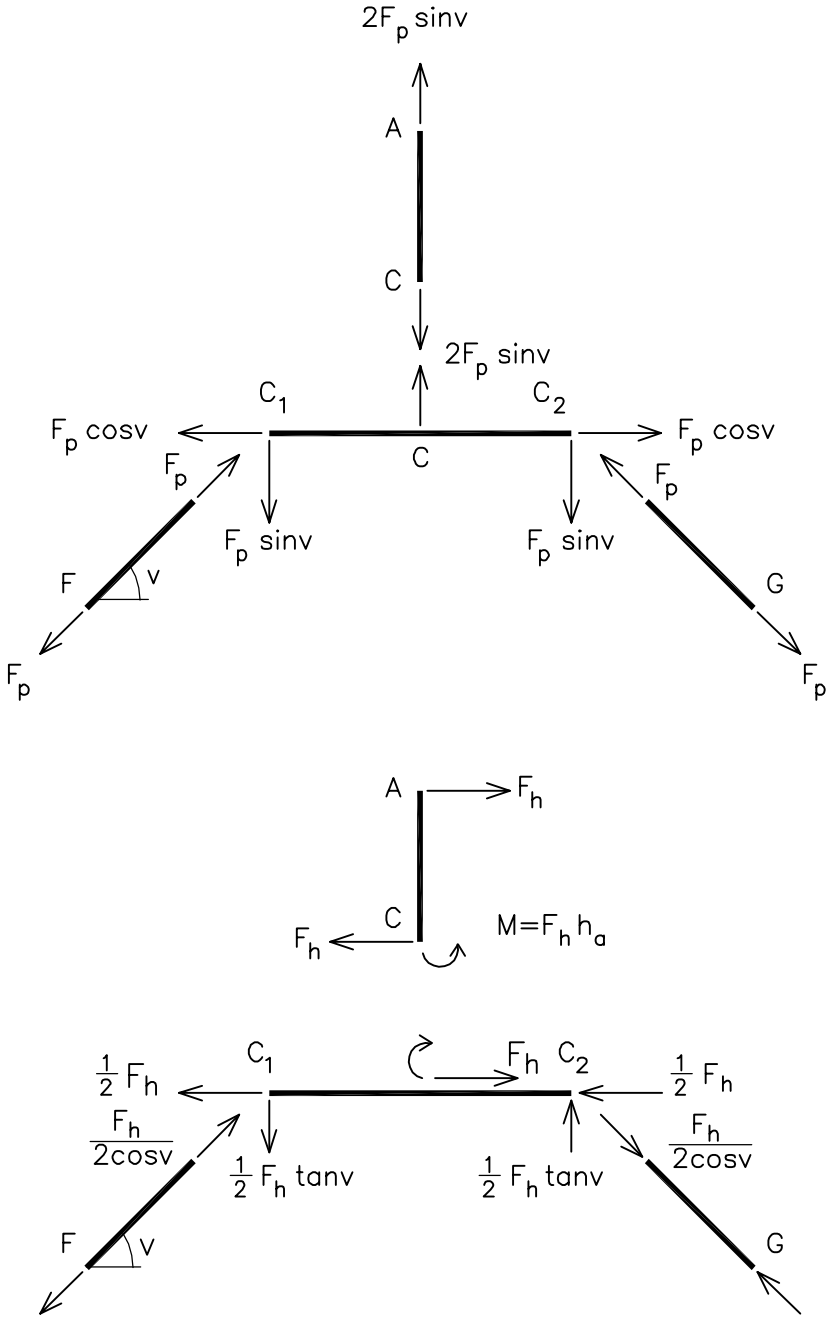

Figure 3. Section forces in damping system.

The frictional moment M_f limits the moment M in the frictional hinge C. For $M = M_f$ is obtained from Figure 3b the antimetrical load contribution to the force in the bars

$$F_a = \frac{M_f}{2h_a \cos v} \tag{3.1}$$

To avoid compression in the bars, they are pretensioned with the same force, i.e.

$$F_p = F_a \tag{3.2}$$

and the maximum force in a bar is then

$$F_{\max} = 2F_a \tag{3.3}$$

giving a necessary cross-sectional area of a bar

$$A_b = \frac{M_f}{\sigma_y h_a \cos v} \tag{3.4}$$

where σ_y is the yield stress of the bar material.

The hinges should not be the weak point in the damping system and especially not the frictional hinge. Then the bolt in the frictional hinge C should be able to transfer a shear force

$$F_{shear} = 2A_b \sigma_y \sin v \tag{3.5}$$

corresponding to a worst case, where both bars yield in tension.

4. RESONANCE LOAD

Here is considered the behaviour of the upgraded frame for a harmonic horizontal load in point A, i.e.

$$F_A(t) = F_{A0} \cos \omega t \tag{4.1}$$

where t is time, F_{A0} the load amplitude and ω the circular load frequency. The structure is considered in the worst case – the resonance case -, where structural stiffness and mass counterbalance each other, such that work done on the structure by the external load must be absorbed by energy dissipation in the structure.

Typically the mass of the damping system is small compared with the mass of the frame and typically the elastic deformations in the damping system are small compared with the deformations from sliding in the frictional hinge of the damping system. Then it is relevant - as done here - to consider the case, where the mass and the elastic deformations of the damping system are neglected. A geometric linear structural theory with undeformed equilibrium is used.

It is assumed that a load cycle causes a displacement cycle, i.e.

$$u_A(t+T) = u_A(t) \tag{4.2}$$

where T is the load period ($\omega T = 2\pi$).

Now the horizontal force F_h in the damping system in point A, see Figure 3b, and the work conjugated displacement u_A can characterize the state in the frictional hinge as shown on Figure 4. Obviously the energy dissipated in the frictional hinge in one cycle is

$$E_f = \frac{4M_f u_{A0}}{h_a} \tag{4.3}$$

where u_{A0} is the displacement amplitude.

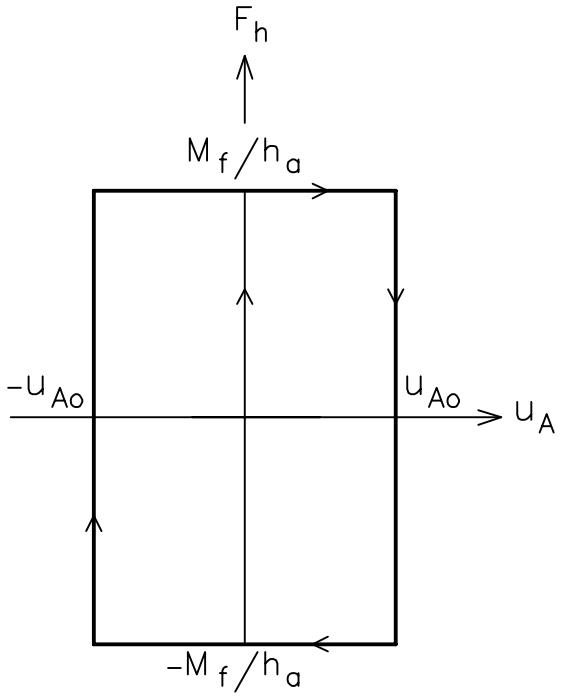

Figure 4. Frictional damping system behaviour.

The work done on the structure by the load F_A is

$$W = \int_0^T F_A(t) du_A \tag{4.4}$$

Approximating $u_A(t) \cong u_{A0} \cos(\omega t + \varphi)$, where φ is the phase, the work W is maximized by $\varphi = -\pi/2$, giving

$$W = \int_0^T F_{A0} \cos \omega t \omega u_{A0} \cos \omega t \, dt = F_{A0} u_{A0} \pi \tag{4.5}$$

Now the energy balance $E_f = W$ gives

$$\frac{M_f}{h_a} = \frac{\pi}{4} F_{A0} \quad and \quad u_{A0} = arbitrary\ value \tag{4.6}$$

Obviously this can be interpreted as: To avoid unlimited response, M_f must be greater than the value determined by (4.6).

5. ELASTIC DEFORMATIONS IN FRICTION DAMPER

The elastic deformations in the friction damping system give a behaviour as indicated in Figure 5, and it is clear from this that these elastic deformations may eliminate the energy dissipation in the damping system.

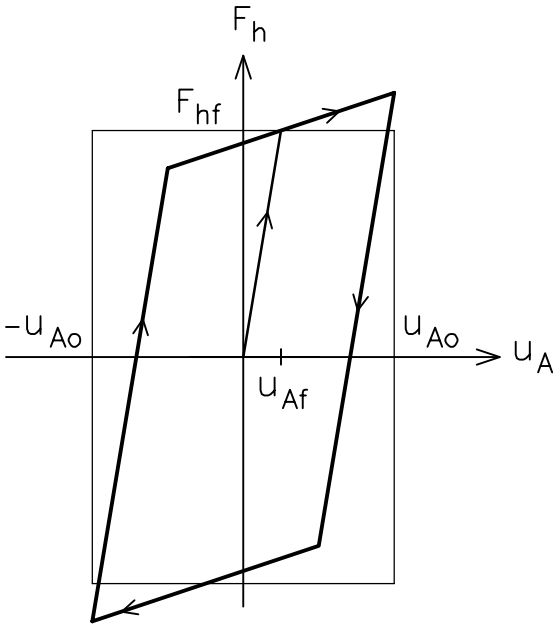

Figure 5. Frictional damping system behaviour.

In order to determine the importance of the elastic deformations in the frictional damping system, the elastic bar deformations are included in the analysis. As in section 3 we consider the behaviour of the upgraded frame loaded by a horizontal load in point A increasing slowly from 0 to F_{A0}. A full geometric linear structural theory is used, i.e. because of the pretension forces, the equilibrium contribution from these has to be established in the deformed state.

Moving point A u_A horizontally and rotating beam AC a and beam C_1CC_2 b as shown on Figure 6 gives the displacements u_{C1} and w_{C1} of point C_1 determined by

$$u_{C1} = u_A - ah_a \qquad w_{C1} = br \tag{5.1}$$

from which the elongation Δl and the slope decrease Δv of bar 1 is determined to

$$\Delta v = ((u_A - ah_a)\sin v + br\cos v)/l \qquad \Delta l = (u_A - ah_a)\cos v - br\sin v \tag{5.2}$$

In (5.1-2) is obviously utilized the assumption of linearity implying restrictions as $|a| << 1$ and $|b| << 1$.

Further, the rotation θ in the frictional hinge C is determined by

$$\theta = a + b \tag{5.3}$$

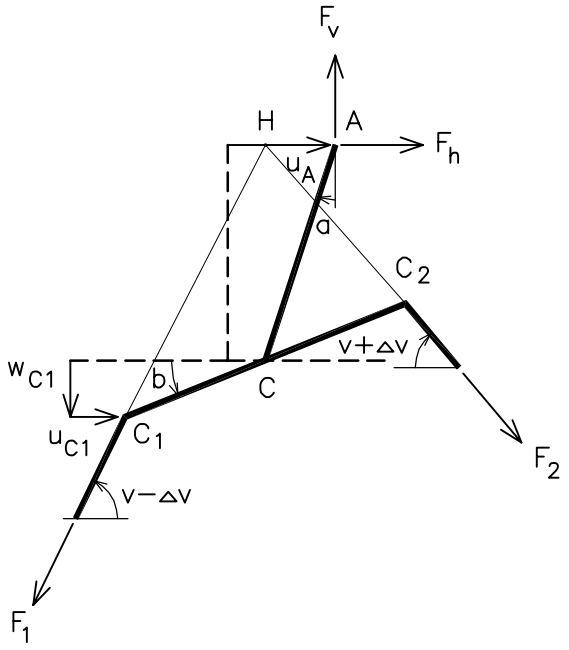

Figure 6. Antimetric deformations in damping system.

Now, because the deformation state characterized by u_A, a and b is antimetric, all other deformation quantities must be antimetric. Then the elongation Δl_i of the two bars (i = 1,2) must be opposite and the slope increases Δv_i too, i.e.

$$\Delta l_1 = -\Delta l_2 = \Delta l \qquad \Delta v_1 = -\Delta v_2 = -\Delta v \tag{5.4}$$

Moreover the antimetry implies that the intersection point between the bar lines A' moves horizontally. Taking the moment about A of the bar forces on the damper, see Figure 6, shows that H must coincide with A. This means that u_A determines the bar slope changes, i.e

$$\Delta v = \frac{u_A \sin v}{L} \tag{5.5}$$

where $L = l + l_a$, see Figure 2. The two expressions (5.2) and (5.5) for Δv gives a deformation constraint between u_A, a and b.

From force equilibrium the horizontal force F_h and the vertical force F_v on the damper in point A are determined by the bar forces F_1 and F_2, see Figure 6

$$\begin{aligned} F_v &= F_1 \sin(v - \Delta v) + F_2 \sin(v + \Delta v) \\ F_h &= F_1 \cos(v - \Delta v) - F_2 \cos(v + \Delta v) \end{aligned} \tag{5.6}$$

The bar force change ΔF from the pretension force is determined by the bar elongation

$$\Delta F = EA_b \frac{\Delta l}{l} \tag{5.7}$$

where E is the Young's modulus for the bar material. Then the bar forces can be written as $F_1 = F_p + \Delta F$ and $F_2 = F_p - \Delta F$ (pretension + antimetric contribution) and the following 1.order approximation for (5.6) is obtained

$$F_v = 2F_p \sin v \qquad F_h = 2\Delta F \cos v + 2\Delta v F_p \sin v \tag{5.8}$$

The final equilibrium condition is the internal moment equilibrium in the damper, e.g. moment about C of AC

$$M = F_h h_a - F_v a h_a \tag{5.9}$$

The equations (5.2,3,5,7,8,9) represent 8 equations with the 9 unknowns a, b, Δv, Δl, θ, F_v, F_h, M and ΔF for specified u_A. The missing equation is dependent on the behaviour in the frictional hinge. In the sticking phase

$$\dot{\theta} = 0 \tag{5.10a}$$

and in the sliding phase

$$M = M_f \tag{5.10b}$$

From (5.2) can a and b be isolated and after elimination of Δv by (5.5) is obtained

$$\begin{aligned} ah_a &= u_A(1-\frac{l}{L}\sin^2 v) - \Delta l \cos v \\ br &= u_A \frac{l}{L}\sin v \cos v - \Delta l \sin v \end{aligned} \tag{5.11}$$

Moreover is obtained from (5.2[2])

$$\Delta l = (u_A - h_a(a+b))\cos v = (u_A - h_a\theta)\cos v \tag{5.12}$$

Also the static/geometric relation between M, θ and u_A is useful. Inserting (5.8), (5.7), (5.5) and (5.12) in (5.9) gives

$$\begin{aligned} M &= \\ & F_h h_a - F_v a h_a = \\ & (2\Delta F \cos v + 2\Delta v F_p \sin v)h_a - 2F_p \sin v a h_a = \\ & (2EA_b \frac{\Delta l}{l}\cos v + 2\frac{u_A \sin v}{L}F_p \sin v)h_a - 2F_p \sin v(u_A(1-\frac{l}{L}\sin^2 v) - \Delta l \cos v) = \\ & \Delta l(2EA_b \frac{h_a}{l}\cos v + 2F_p \sin v \cos v) + u_A F_p(2\frac{h_a}{L}\sin^2 v - 2\sin v(1-\frac{l}{L}\sin^2 v)) = \\ & u_A(2EA_b \frac{h_a}{l}\cos^2 v + 2F_p(\sin v \cos^2 v + \frac{h_a}{L}\sin^2 v - \sin v(1-\frac{l}{L}\sin^2 v))) - \\ & \quad \theta h_a \cos^2 v(2EA_b \frac{h_a}{l} + 2F_p \sin v) = \\ & u_A 2EA_b \frac{h_a}{l}\cos^2 v - \theta h_a \cos^2 v(2EA_b \frac{h_a}{l} + 2F_p \sin v) \end{aligned} \tag{5.13}$$

This expression for θ is compared on Figure 7 with the geometrical exact θ from [1] and the results indicate that the accuracy of the geometric linear theory is high.

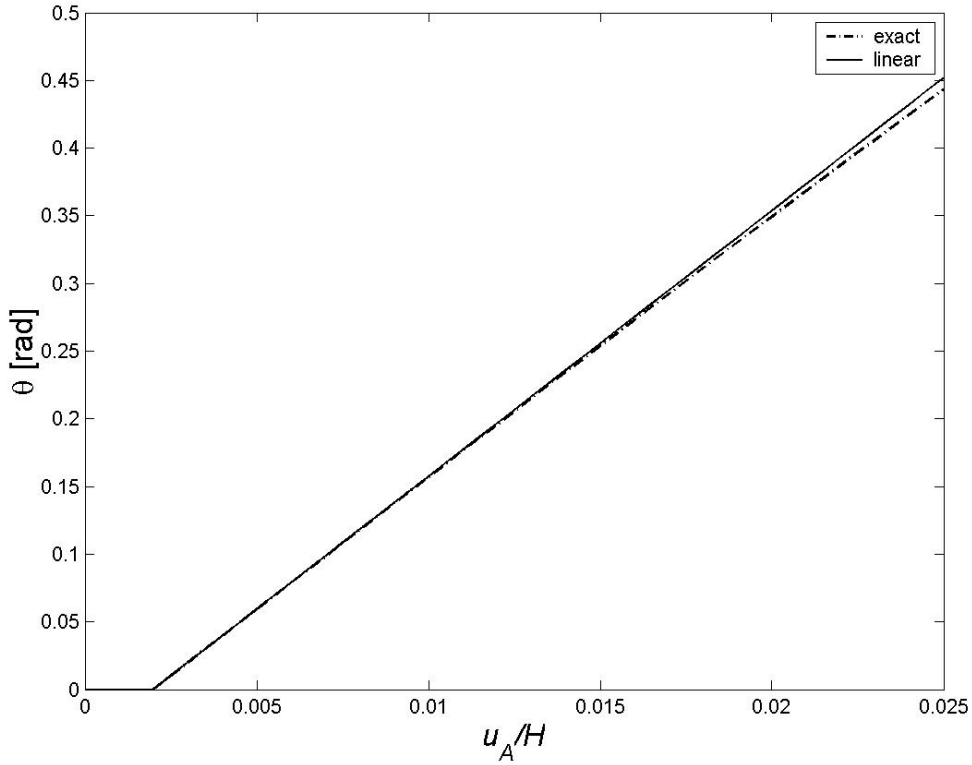

Figure 7. $\theta(u_A)$ based on geometrical linear respectively exact theory for a frame with damping system defined by $tan v$=4/3, F_p/EA_b=1'-3, M_f/h_aEA_b= 1.2'-3 and h_a/H=1/20.

Sticking phase

Up to a certain load level no sliding occurs in the frictional hinge. In this sticking phase $\theta = 0$ and then (5.12) gives

$$\Delta l = u_A \cos v$$

(5.11) and (5.5) then gives

$$a = -b = \Delta v \tag{5.14}$$

The horizontal stiffness K_{bd} of the damping system in the sticking phase defined by

$$F_h = K_{bd} u_A \tag{5.15}$$

is easily obtained from (5.8[2])

$$K_{bd} = \frac{2EA_b}{l}\cos^2 v + \frac{2F_p}{L}\sin^2 v \tag{5.16}$$

Typically the last term - the geometric term - in (5.16) is small compared with the first term – the stiffness term. This is easily seen using the design from section 3

$$last\,term\,/\;first\,term = \frac{\sigma_y}{E}\frac{l}{2L}\tan^2 v \approx 2'\text{–}3$$

because $l\tan^2 v/2L \approx 1$ for typical frame geometries and $\sigma_y / E \approx 0.002$ for typical bar materials.

The sticking phase finishes, when the moment in the frictional hinge reaches the frictional moment. From (5.9) is obtained the value u_{Af} for u_A for which sticking finishes

$$u_{Af} = \frac{M_f l}{2h_a EA_b \cos^2 v} \tag{5.17}$$

Obviously u_{Af}/u_{A0} represents the relative reduction in energy dissipation in the frictional hinge, see Figure 5. In order to be specific the design from section 3 is used. Then

$$u_{Af} = \frac{\sigma_y}{E} H \frac{l}{2H\cos\nu} \approx 2'\text{–}3H \tag{5.18}$$

for typical frame geometries and for typical bar materials. Because typical design values are $u_{A0} \approx 0.005H - 0.01H$, (5.18) shows that the elastic deformations in the bars give only a minor reduction of the energy dissipation in the friction damping system. However, if the elastic deformations in the bars are too large in other cases, the bar cross sectional area A_b must be increased.

Sliding phase

In the sliding phase following the initial sticking phase $M = M_f$ and then (5.9) after some manipulations gives an expression for determination of a

$$a(\frac{h_a}{l} + \frac{F_p}{EA_b}\sin\nu) = -\frac{M_f}{2EA_b h_a} + \frac{u_A}{l}(1-(1-\frac{F_p}{EA_b})\frac{l}{L}\sin^2\nu) \tag{5.19}$$

For changes in the sliding phase, (5.9) gives

$$0 = h_a dF_h - F_v h_a da$$

i.e.

$$K_{bd} = \frac{dF_h}{du_A} = \frac{dF_h}{da}\frac{da}{du_A} = F_v \frac{da}{du_A}$$

Combining this with (5.19), is obtained for K_{bd} in the sliding phase

$$K_{bd} = \frac{2F_p}{l}\sin\nu \frac{1-(1-\frac{F_p}{EA_b})\frac{l}{L}\sin^2\nu}{\frac{h_a}{l} + \frac{F_p}{EA_b}\sin\nu} \tag{5.20}$$

Comparing this expression for the stiffness K_{bd} with the sticking phase expression (5.16) shows that the stiffness in sliding phase typically is much smaller than in the sticking phase. With the non-dimensional horizontal force $F_h^* = \frac{F_h}{M_f / h_a}$ in the damping system, the nearly bilinear behavior of the damping system in the typical displacement domain $u_A < 0.01H$ is illustrated on Figure 8.

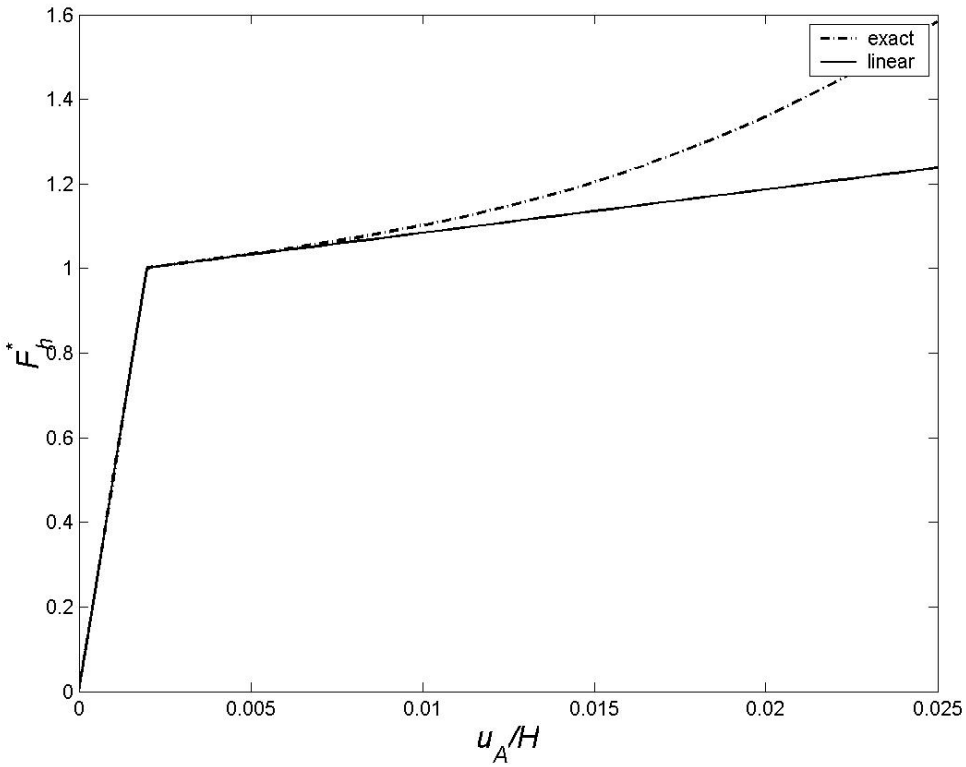

Figure 8. $F_h^*(u_A)$ based on geometrical linear respectively exact theory for a frame with damping system defined by $tanv$=4/3, F_p/EA_b=1'-3, M_f/h_aEA_b= 1.2'-3 and h_a/H=1/20.

Key parameters

Typically

$$\frac{F_p}{EA_b} << 1 \tag{5.22}$$

Then (5.15), (5.16) and (5.20) give

$$F_h^* = \begin{cases} u_A^* & sticking \\ 1 & sliding \end{cases} \tag{5.23}$$

where the non-dimensional displacement is defined by $u_A^* = u_A / u_{Af}$. The behavior of the frictional damping system is then of elastic, perfectly plastic type. Moreover is seen from (5.23) that the parameters, which determine the action from the damping system on the frame, are the force scale M_f/h_a and the displacement scale u_{Af} of the damping system.

Energy dissipation

Neglecting the small horizontal stiffness of the damping system in the sliding phase, the energy dissipation per cycle in the frictional hinge can with $F_{hf} = K_{bd} u_{Af}$ be written as, see Figure 5

$$E_f = 4F_{hf}(u_{A0} - u_{Af}) = 4K_{bd} u_{Af}(u_{A0} - u_{Af}) \tag{5.24}$$

which for constant K_{bd} is maximized by $u_{Af} = \frac{1}{2} u_{A0}$. Because K_{bd} is independent of M_f, this result and (5.17) allow introduction of an energy dissipation optimized frictional moment M_{fopt} determined by

$$\frac{M_{fopt}}{h_a E A_b} = \frac{u_{A0}}{l}\cos^2 v \tag{5.25}$$

The energy dissipation optimized design defined by (5.25) may correspond to bars of insufficient strength. If this is the case, the bar cross sectional area A_b has to be increased to a sufficient value as indicated in section 3. This A_b-increase has nearly no influence on F_{hf}, see (5.16-17), and decreases u_{Af}, see (5.17), i.e. E_f is increased, see (5.24), but of course not so much as for an energy dissipation optimized design.

Design

As an example, the design procedure is indicated for the resonance problem, see section 4.

a. The frame geometry, the bar material and the load is given, i.e. H, S, E, F_{A0}.
b. u_{A0} is given, e.g. $0.01H$.
c. The damper is assumed small, i.e. $l \cong L$.
d. (4.6) determines a value for M_f/h_a and with this value for M_{fopt}/h_a, (5.25) gives a value for A_b. Also (3.4) gives a value for A_b and the larger of these two (typically the latter) must be used.

The above procedure determines only the ratio M_f/h_a and not both M_f and h_a. Of course a small damper is advantageous in regard to material consumption, extra load on the structure and damper installation. However, the damper has to be so large that it is possible to produce it with nearly rigid beams and space for the connection holes. Moreover, the rotation θ in the frictional hinge should be limited in order to reduce wear and temperature increases in the hinge. An upper bound for θ gives a lower bound for the damper size. Then, with a reasonable value for h_a, M_f is determined.

The above theory is not valid for large rotations in the damper.

6. NON-CENTRAL DAMPING SYSTEM

Here is considered the case, where the intersection point H between the bar lines, see Figure 9, is not coincident with the connection point A, i.e. the damping system is non-central. Still defining the frame geometry by H and S and the damper geometry by h_a and r, suitable auxiliary geometric quantities are defined as follows. The bar slope angle v

$$\tan v = \frac{H - h_a}{S/2 - r} \tag{6.1}$$

, the bar length

$$l = \sqrt{(S/2 - r)^2 + (H - h_a)^2} \tag{6.2}$$

, the eccentricity of the bar lines intersection point

$$h_h = \frac{S}{2}\tan v - H \tag{6.3}$$

, the length of the bar line from support to intersection point

$$L = \sqrt{(S/2)^2 + (H + h_h)^2} \tag{6.4}$$

and the length of the damper projection perpendicular on a bar

$$d = r\sin v - h_a \cos v \tag{6.5}$$

h_h and d are positive, if the intersection point H is above the connection point A, and negative, if the intersection point is below the connection point.

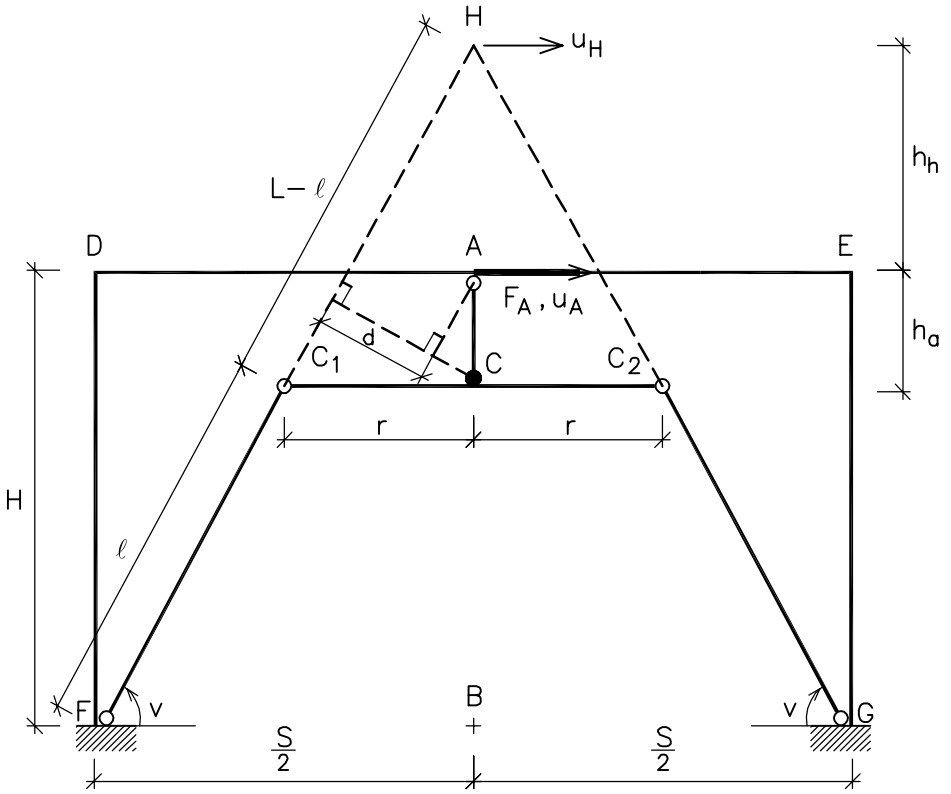

Figure 9. Frame with non-central damping system.

As in section 5 a full geometric linear structural theory is used. The behavior is still antimetric and the damper behavior is still as shown on Figure 6. Then the equations (5.2), (5.3), (5.4), (5.7), (5.8), (5.9) (5.10a,b) are still valid, but (5.5) must be replaced by

$$\Delta v = \frac{u_H \sin v}{L} \tag{6.6}$$

and the moment equation about the connection point A in the deformed state, see Figure 10, now gives

$$F_v(u_A - u_H) + F_h h_h = 0 \tag{6.7}$$

Applying (5.8), (6.6) and (5.7), (6.7) is transformed to an equation in Δv and Δl

$$F_p \sin v(u_A - \frac{\Delta v L}{\sin v}) + h_h(\frac{EA_b}{l}\Delta l \cos v + \Delta v F_p \sin v) = 0 \tag{6.8}$$

From (5.2) are obtained expressions for *a* and *b*

$$ah_a = u_A - \Delta v l \sin v - \Delta l \cos v \qquad br = \Delta v l \cos v - \Delta l \sin v \tag{6.9}$$

and then

$$\theta = a + b = (u_A - \Delta v l \sin v - \Delta l \cos v)/h_a + (\Delta v l \cos v - \Delta l \sin v)/r \tag{6.10}$$

Now the initial sticking phase is analyzed in the typical case

$$EA_b >> F_p \tag{6.11}$$

and it is assumed that the damping system is not nearly central, i.e. h_h and d not very close to 0.

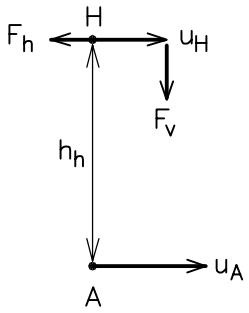

Figure 10. The bar forces F_1 and F_2 are referred to the intersection point H and then expressed by F_h and F_v.

Because of the assumption (6.11), (6.8) gives $\Delta l/l << \Delta v$. Then (6.10) gives

$$u_A = \Delta v \frac{ld}{r} \tag{6.12}$$

Eliminating u_H from (6.7) with (6.6) and next Δv with (6.12), we obtain

$$F_h = \frac{2F_p \sin v}{h_h} u_A (-1 + \frac{rL}{ld \sin v})$$

which determines the damper system stiffness in the sticking phase to

$$K_{bd} = \frac{2F_p \sin v}{h_h} (-1 + \frac{rL}{ld \sin v}) \tag{6.13}$$

If the damping system is under-central, then $h_h<0$ and $d<0$ and (6.13) gives a positive value for K_{bd}. For an over-central system $r>d>0$ and $L>l$. Then the parenthesis in (6.13) is positive and because h_h now is positive, K_{bd} is positive too.

Comparing (6.13) with a F_p factor and (5.16) with a EA_b factor shows that in the sticking phase is K_{bd} typically much smaller for the non-central damping system than for the central.

The expression for K_{bd} in the sticking phase (6.13) is compared with the geometric exact solution on Figure 11. One sees that a geometric linear theory is insufficient already in the sticking phase.

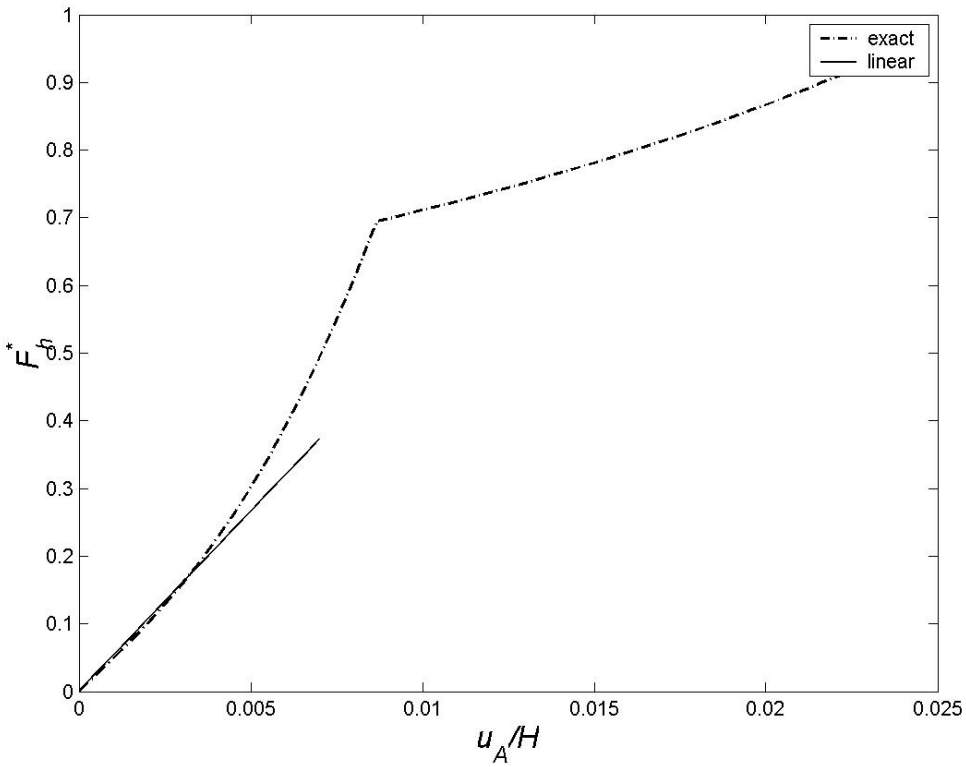

Figure 11. $F_h^*(u_A)$ based on geometrical linear respectively exact theory for a frame with non-central damping system defined by $H/(S/2)=4/3$, $h_a/r=2/3$, $F_p/EA_b=1$'-3, $M_f/h_aEA_b=$ 1.2'-3 and $h_a/H=1/20$.

7. CONCLUSIONS

It is shown that the damping system can be designed such that it is able to dissipate energy efficiently in dynamic loaded building structure in spite of severe displacement limitations for such structures.

An energy dissipation optimized design is introduced. This determines the frictional moment, but gives typically unsafe values for some other design variables. It is specified how these must be modified.

A rather accurate bilinear approximation for the behavior of the central damping system is determined. Utilizing this and not the full non-linear behavior of the damping system for numerical computations can highly improve the efficiency of such computations.

Typically the non-central damping system has a stiffness much smaller than the central damping system and moreover it cannot be modeled accurately as a bilinear system.

REFERENCES

1. Mualla IH. *Experimental & Computational Evaluation of a New Friction Damper Device*. Ph.D. thesis, Dept. of Structural Engineering and Materials, Technical University of Denmark, 2000.
2. Skinner RI, Robinson WH and McVerry GH. *An Introduction to Seismic Isolation*. John Wiley & Sons. 1993.
3. Filiatrault A and Cherry S. 'Seismic design spectra for friction-damped structures' *Journal of Structural Engineering* 116(5), 1334-1355 (1990).